SUBREGIONS OF MOTION AND ELLIPTIC HALO ORBITS IN THE ELLIPTIC RESTRICTED THREE-BODY PROBLEM

Stefano Campagnola [*] **, Martin Lo** [†] **and Paul Newton** [‡]

In this paper we present regions of motion and periodic orbits in the spatial elliptic restricted three body problem (ER3BP). Periodic orbits and regions of motion are fundamental keys to understand any dynamical system; for this reason the Hill's surfaces or the families of halo orbits have been extensively studied in the frame of the circular restricted three body problem. It is our opinion that their natural extensions to the ER3BP have not been studied enough. We divide the position space into forbidden subregions, subregions of motion and low-velocity subregions. We use these notions to define necessary condition for a transfer trajectory in the ER3BP. Also we compute branches of elliptic halo orbits bifurcating from halo orbits in the circular restricted three body problem. The new periodic orbits have principal periods and stability properties different from those of the originating halo orbit.

INTRODUCTION

In the last decades, several authors studied low-energy transit trajectories to achieve large saving in fuel costs or to provide a temporarily stable orbit in case of failure of the orbit insertion.[1] In many cases the model of the circular restricted three-body problem (CR3BP) was used to explore the solution space,[2] and inspired very challenging mission design.

The CR3BP studies the motion of an infinitesimal body under the gravitational attraction of two massive bodies (primaries) in circular motion around their center of mass. Choosing a rotating reference frame that keeps the position of the primaries fixed results in a set of autonomous ordinary differential equations. The dynamical system is Hamiltonian with the Hamiltonian as integral of motion. The existence of a first integral helps define regions of motion and families of periodic orbits with their stable and unstable manifolds. Those are key elements to understand any dynamical system.

However, the motion of the planets in the solar system is better approximated by elliptic orbits, with eccentricity varying from 0.01 up to 0.2 (for the Sun-Mercury system). The elliptic restricted three-body problem (ER3BP) takes into account the eccentricity of the orbit of the primaries, and it is therefore a more accurate model than the CR3BP. Yet the ER3BP has not been studied much, because it is a more complex system than the CR3BP. The equations of motion of the ER3BP are non-autonomous because the distance between the primaries varies in time. The system does not possess an integral of motion (although it may when averaged appropriately[3]), which suggests that the ER3BP is a dynamical problem different from the CR3BP.

For instance, the CR3BP model allows one to compute families of periodic orbits, although no real periodic orbit exists in the real solar system. The ER3BP shows that only discrete periodic or-

[*]Ph.D. student, Aerospace and Mechanical Engineering, University of Souther California, Los Angeles, Ca 90089.

[†]Jet Propulsion Laboratory, California Institute of Technology, Pasadena , CA 01109.

[‡]Aerospace and Mechanical Engineering, University of Souther California, Los Angeles, Ca 90089.

bits exist for $e \neq 0$, with a well determined period, rather than families with continuously varying periods. These solutions are (almost) periodic also in the ephemeris model: Figure 1 shows a periodic orbit in the sun-Mercury system, integrated in the ER3BP (solid line) and in the full ephemeris (dotted line, one dot per day). We call this periodic orbit an elliptic halo orbit since it is computed from continuation of a halo orbit in the CR3BP into the ER3BP.
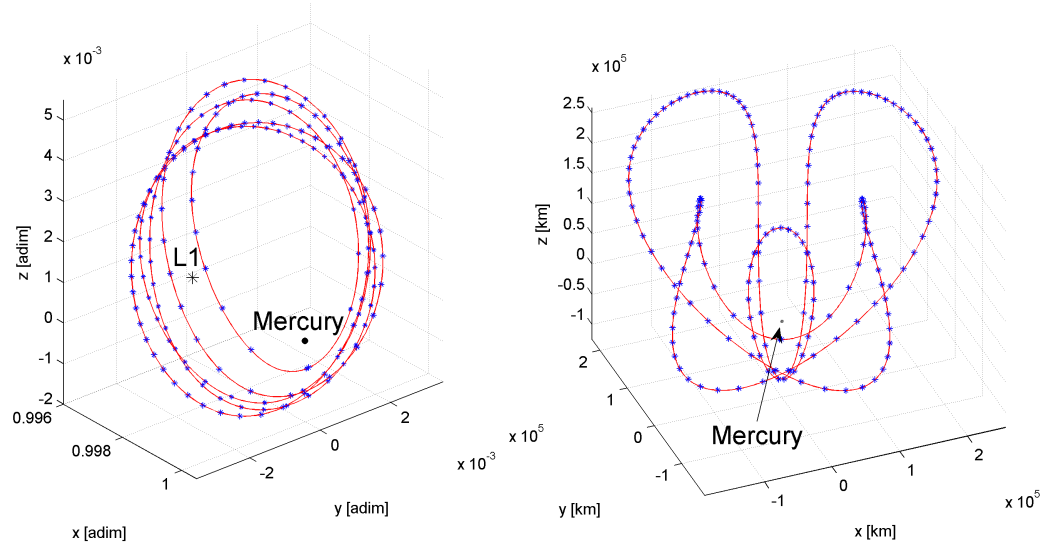

Figure 1 **Periodic orbit in the Sun-Mercury system. We call these orbits *elliptic halo orbits*, as they are computed starting from halo orbits in the CR3BP . The left plot is in the rotating reference frame, the right plot is in the Mercury equatorial reference frame. the mercury equatorial reference frame is an inertial frame centered in Mercury. The solid line is the trajectory integrated in the ER3BP, the dotted line is the trajectory integrated with full ephemeris (one dot per day). This shows the ER3BP is a very accurate model for trajectories in the Sun-Mercury system.**

The ER3BP should be used in the preliminary or PhaseA space mission trajectory design, if the eccentricity of the system under study is too large to use the CR3BP. Trajectories like the Bepi-Colombo gravitational capture at Mercury are designed in the ER3BP and are explained using manifolds of quasi-periodic orbits in the ER3BP[4] (Figure 2).

In an effort to better understand the differences between the CR3BP and the ER3BP, this paper describes some of the important feature of the ER3BP: regions of motion and periodic orbits. The main approach consists in considering the eccentricity e as a continuation parameter: For $e = 0$ the equations of motion reduce to the CR3BP.

The first section briefly recalls the regions of motion and the periodic orbits in the CR3BP. In the second section we introduce the equations of motion of ER3BP isolating the terms containing the eccentricity. In the third section we discuss the properties of the pulsating zero-velocity surfaces and define new subregions of motion for the elliptic problem. The forbidden subregions, subregions of motion and low-velocity subregions are bounded by pulsating surfaces. In the last section we compute branches of periodic orbits at different e, bifurcating from special halo orbits in the CR3BP. We show that the stability properties change as soon as $e \neq 0$, and we believe that a countable infinity of bifurcations occur at $e = 0$, filling the bifurcation diagram with infinitely many (although discrete) branches. This provides some insight on the existence and stability of the quasi-periodic halo orbits in the full ephemeris model.
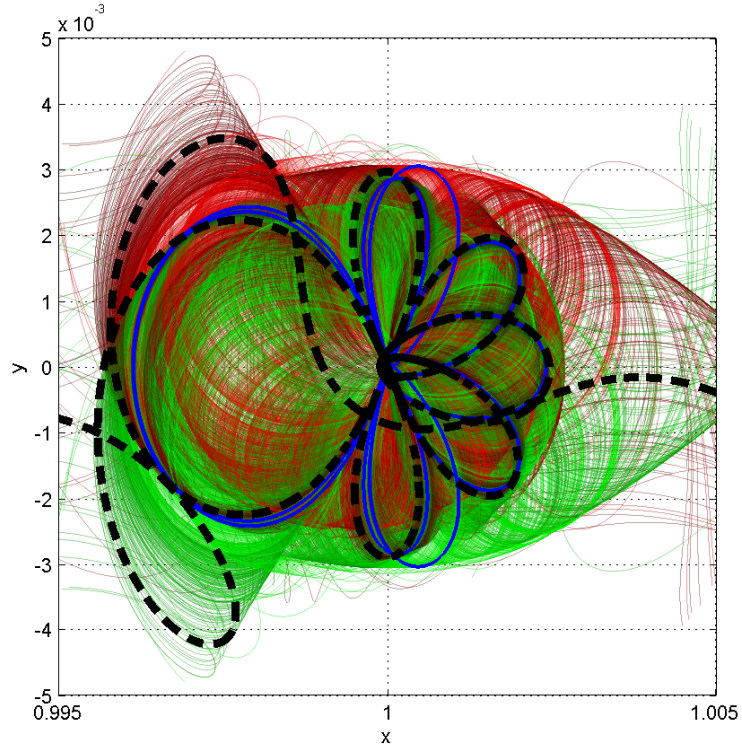
Figure 2 **The BepiColombo gravitation capture trajectory at Mercury shadows manifolds of quasi-periodic orbits in the elliptic restricted three-body problem (ER3BP).[4] In this xy projection in the rotating reference frame, the BepiColombo trajectory is the bold dash curve, the quasi periodic orbit is the bold solid curve, and the manifolds are the thin curves. A better understanding of the key feature of the ER3BP helps designing missions for planets like Mercury.**

BACKGROUND

In this section we briefly recall some key features of the circular restricted three body problem.[5] In the *general* restricted three-body problem, an infinitesimal particle m_3 moves under the gravitational attraction of two primaries m_1 and m_2 ($m_3 \ll m_2 < m_1$), without affecting them. The motion of m_3 is usually described in a special reference frame, where the position of the primaries is fixed along the $x - axis$ (also called the $syzygy$ axis) and their mutual distance is normalized to 1; the z-axis is perpendicular to the primary orbit, and we call the xz plane the *normal plane*.

Finally, when writing the equations of motion the true anomaly of the primaries is the preferred independent variable instead of time.

In the *circular* restricted three body problem (CR3BP), the primaries moves on circular orbits, and the motion of m_3 is the solution of the following autonomous system of ordinary differential equations (ODEs):

$$\begin{cases} \ddot{x} - 2\dot{y} &= \frac{\partial \Omega_C}{\partial x} \\ \ddot{y} + 2\dot{x} &= \frac{\partial \Omega_C}{\partial y} \\ \ddot{z} &= \frac{\partial \Omega_C}{\partial z} \end{cases} \tag{1}$$

with

$$\Omega_C(x, y, z) \equiv \frac{1}{2}\left(x^2 + y^2\right) + \frac{1-\mu}{r_1} + \frac{\mu}{r_2} + \frac{1}{2}(\mu - 1)\mu$$

where $r_1 = \sqrt{(x - \mu)^2 + y^2 + z^2}$ and $r_1 = \sqrt{(x - \mu + 1)^2 + y^2 + z^2}$ are the distances to the primaries, and $\mu = m_2/m_1$ is the mass parameter.

The system has five fixed points $\mathbf{x_{Li}}, i = 1, \ldots 5$, the Lagrangian points (also called Libration points). The positions of the Lagrangian points depend on the parameter μ. The system also possesses one integral of motion, the Jacobi constant [*]:

$$J_C = 2\Omega_C - V_C^2 \tag{2}$$

where $V^2 = \left(\dot{x}^2 + \dot{y}^2 + \dot{z}^2\right)$.

Transfer trajectories are possible only if $J_C < J_{L1}$, where $J_{L1}(\mu)$ is the Jacobi constant associated to the first Libration point.

Zero Velocity Surfaces

Hill used Eq. (2) to define zero-velocity surfaces which separate regions of motion from the forbidden regions.[6] Given a set of initial condition $(t_0, \mathbf{x_0})$, Hill's zero-velocity surfaces are level sets of $2\Omega_C$:

$$2\Omega_C = J_C(\mathbf{x_0})$$

If the initial conditions are such that $J_C < 3$, the motion of the third body in the xy plane is unbounded. If the initial conditions are such that $J_C > J_{L1}$, the motion of the third body is bounded around either of the primary, or far away from both. Figure 3 shows the zero-velocity surfaces for the Pluto-Charon system.

Periodic Orbits

A fundamental step in understanding any dynamical system is to identify its periodic orbits and classify their linear and nonlinear stability.[7] For a fixed value of the mass parameter μ, the CR3BP possesses *families* of periodic orbits parametrized by the Jacobi constant J_C, as implied by the Cylinder Theorem:[8]

> An elementary periodic orbit of a system with an integral I lies in a smooth cylinder of solutions parametrized by I.

---

[*]The Hamiltonian $\mathcal{H}$, which is time-independent and is therefore an integral of motion, is related to the Jacobi constant: $2\mathcal{H} = -J_C + \mu(1 - \mu)$.
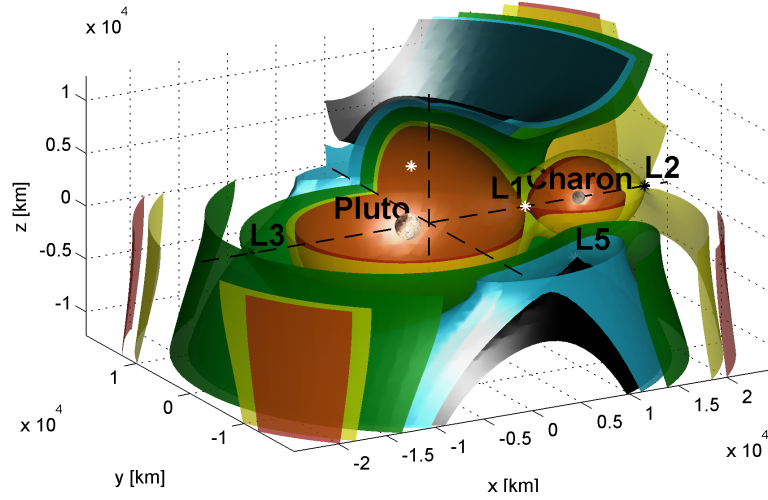
Figure 3   Level sets of the function 2Ω in the Pluto-Charon system ($\mu \simeq 0.123$). In the circular restricted three-body problem, the level sets are the Hill's zero-velocity surfaces, and separate regions of motion from the forbidden regions.

Several authors computed families of periodic orbits in the CR3BP.[9, 10, 11, 12, 13] In this work we use orbits of the halo orbit families. Their linear stability is determined by computing the linear map

$$\varphi_C : \delta\mathbf{x}(t_0) \rightarrow \delta\mathbf{x}(T + t_0) = M\delta\mathbf{x}(t_0)$$

between consecutive crossings through a Poincaré section. Here $\delta\mathbf{x}(t_0)$ is an arbitrary initial perturbation of the state $\mathbf{x} = [x, y, z, u, v, w]$, M is the monodromy matrix and T is the principal period of the orbit. The stability of the map φ, and hence of the orbit, is related to the eigenvalues λ of the monodromy matrix M: eigenvalues inside the unit circle ($\lambda < 1$) are associated to the stable manifold W_s ; eigenvalues outside the unit circle are associated to the unstable manifold W_u ; and pure imaginary eigenvalues are associated with tori of quasi periodic orbits.

In the restricted three-body problem, the eigenvalues λ of the monodromy matrix come in reciprocal pairs, so that the periodic orbit is linearly stable if and only if all the eigenvalues are on the unit circle. Also, in the CR3BP two eigenvalues are real unitary, and are associated to eigenvectors $\delta\mathbf{x}_0$ tangent to the trajectory: because the system is autonomous, such perturbation corresponds to a small phase change along the orbit.

SPATIAL ELLIPTIC RESTRICTED THREE-BODY PROBLEM

In the elliptic restricted three body problem the two primaries move on elliptic orbits around their barycenter. Unlike the CR3BP, the ER3BP is a non-autonomous system of ODE's. The eccentricity e of the orbit of the primaries appears as a parameter. The motion of the third body m_3 is usually described in a pulsating reference frame, where the position of the primaries is fixed along the $x - axis$ (the $syzygy$ axis) and their mutual distance is normalized to 1; as in the CR3BP, we define the the *normal plane* as the plane throught the x-axis perpendicular to the primary orbit. Again, the true anomaly of the primaries is the preferred independent variable instead of time. The system of ODE's can be written in the following form:

$$\begin{cases} \ddot{x} - 2\dot{y} = \frac{\partial \Omega_C}{\partial x} - \frac{e\cos f}{1+e\cos f}\frac{\partial \Omega^*}{\partial x} \\ \ddot{y} + 2\dot{x} = \frac{\partial \Omega_C}{\partial y} - \frac{e\cos f}{1+e\cos f}\frac{\partial \Omega^*}{\partial y} \\ \ddot{z} = \frac{\partial \Omega_C}{\partial z} - \frac{e\cos f}{1+e\cos f}\frac{\partial \Omega^*}{\partial z} \end{cases} \tag{3}$$

$$\Omega^*(x,y,z) = \Omega_C + \frac{1}{2}z^2$$

Here we isolated the term $\frac{e\cos f}{1+e\cos f}$ which is the only one containing the independent variable as well as the eccentricity. For $e = 0$, the equations of motion of the ER3BP reduce to Eq. (1); therefore solutions of the CR3BP are also solutions of the ER3BP when the eccentricity vanishes. In fact we will show that some special solutions of the CR3BP can be continued to the ER3BP using the eccentricity as continuation parameter, and that a bifurcation occurs at $e = 0$.

The Lagrangian points are also fixed points for the ER3BP. However, it is not possible to find an integral of motion because the equations of motion (and the Hamiltonian $\mathcal{H}$) depend explicitly on the independent variable f. The constant of integration, which was the Jacobi constant in the CR3BP, is now replaced by:

$$J_E = 2\Omega_C - V^2 - (A + I) = J_C - (A + I) \tag{4}$$

where we introduced an integral term I and a pulsating term $A^\dagger$

$$I = 2\int_{f_0}^{f} \Omega^* \frac{e\sin f}{(1 + e\cos f)^2} df$$

$$A = 2\Omega^* \frac{e\cos f}{1 + e\cos f}$$

Note that J_E is not an integral of motion for the ER3BP as it is no longer constant along a trajectory, but depends on the initial $\mathbf{x}(t_0)$ and the initial true anomaly, f_0. However, Eq (4) is actually a function f as well. The interesting thing is that $J_E(f_0, \mathbf{x}(f_0), f)$ is a constant, equal to $J_E(f_0, \mathbf{x}(f_0), f)$. However, choosing different initial conditions within the same trajectory results in different J_E's: we cannot uniquely associate a trajectory to a single value of J_E. This is one of the important consequence of the loss of the integral of motion in the ER3BP when $e \neq 0$. In the rest of the paper we will discuss how this loss affects the forbidden regions and the periodic orbits.

---

† In literature:

$$\begin{cases} x'' - 2y' = \frac{\partial \omega_E}{\partial x} \\ y'' + 2x' = \frac{\partial \omega_E}{\partial y} \\ z'' = \frac{\partial \omega_E}{\partial z} \end{cases}$$

with $\omega_E(x,y,z,f;e) = \frac{\Omega_E}{1+e\cos(f)}$ and $\Omega_E(x,y,z,f;e) = \frac{1}{2}\left(x^2 + y^2 - z^2 e\cos f\right) + \frac{1-\mu}{r_1} + \frac{\mu}{r_1} + \frac{1}{2}\mu(1-\mu)$.

Also the constant of integration is commonly expressed as $J_E = 2\omega_E - V^2 - 2e\int_{f_0}^{f} \Omega_E \frac{\sin f}{(1+e\cos f)^2} df - 2e\int_{f_0}^{f} \frac{z^2 \sin f}{(1+e\cos f)}$, so that by comparing with Eq. (4): $I \equiv 2e\int_{f_0}^{f} \Omega_E \frac{\sin f}{(1+e\cos f)^2} df + 2e\int_{f_0}^{f} \frac{z^2 \sin f}{(1+e\cos f)}$ and $2\Omega_C - A \equiv 2\omega_E$

SUBREGIONS OF MOTION

From the definition of the constant of integration J_E, the velocity squared is given by:

$$V^2 = 2\Omega_C - A - I - J_E$$

Given a set of initial condition , zero-velocity surfaces in the ER3BP are the level sets of the function:

$$2\Omega_C - A - I = J_E(f_0, \mathbf{x_0}) \tag{5}$$

The forbidden region is the set $\mathcal{F}_f = \{(x, y, z) | (2\Omega_C - A - J_E) < I\}$ and the region of motion is the set $\mathcal{A}_f = \{(x, y, z) | (2\Omega_C - A - J_E) > I\}$, where the subscript f indicates that the set changes with the true anomaly.

In this section we discuss the quasi-steady approach, first proposed by Szebehely[5] to compute approximate zero-velocity surfaces, and then introduce an alternative approach leading to the definition of subregions of motions.

Pulsating Zero-Velocity Surfaces

Because of the integral term I, Eq. (5) cannot be solved for (x, y, z) at a time $f_1 \neq f_0$. The *quasi-steady* approach neglects the integral term when $|f_1 - f_0| = \delta f$ is sufficiently small. The quasi-steady approach was formulated for the planar ER3BP and it is often used assuming small out-of-plane motion. Eq. (5) then becomes

$$\frac{2\Omega_C}{1 + e\cos(f)} = 2\Omega_C - A = J_E$$

At each instant $f^* \in [f_0, f_1]$, the level set of $2\Omega_C = J_E(1 + e\cos f^*)$ defines new zero-velocity surfaces[‡]. Because of the $\cos f*$ term, these surfaces get closer and further to the primaries (in the non-dimensional reference frame) as the true anomaly f goes from $-\pi$ to π. Thus they are usually referred to as *pulsating* zero-velocity surfaces.

Yet even for very small δf the quasi-steady approach can result in very large errors. Figure 4 shows an orbit with period 2π in the Sun-Mercury ER3BP. At $f_0 = \pi$ the third body is on the x-axis with zero velocity; thus the initial zero-velocity surfaces include the initial position. After just a few instants, the zero-velocity surfaces shrinks to half their initial initial sizes, and the forbidden regions now include the instantaneous third body location.

Figure 5 explains this paradox showing that the neglected integral term I (computed numerically) is of the same order of magnitude of the pulsating term A; in fact the two terms almost cancel each other out. This suggests that at least in some cases the pulsating behavior is a spurious consequence introduced by the approximation.

When the third body is at equilibrium , for instance, the zero-velocity surface is the invariant set containing the equilibrium point. At any instant f the integral term I and the pulsating term A cancel

---

[‡]For $z \neq 0$ the zero-velocity surfaces are the level sets of $2\Omega_C - z^2 e\cos f^* = J_E(1 + e\cos f^*)$
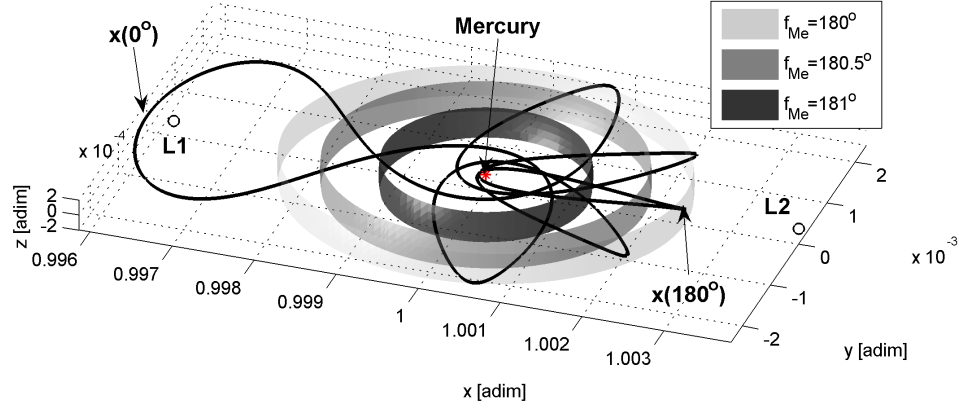
Figure 4   Pulsating zero-velocity surfaces in the Sun-Mercury system. f_{Me} **is the true anomaly of Mercury. At time** $f_{Me} = 180^o$ **the initial velocity is zero; the zero-velocity surfaces are tangent to the initial point. However, after just a few instant the pulsating surfaces have shrunken to half their size, while the third body has barely moved.**
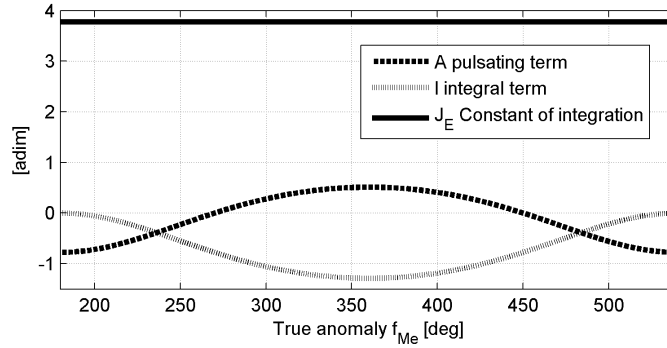
Figure 5   The integral term I **(numerically computed) and the pulsating term** A **of the constant of integration** J_E **for the periodic orbit of Figure 4 as function of the true anomaly of Mercury. When summed together, the integral term almost cancel the pulsating term. Neglecting the integral term results in a large artificial pulsation of the constant of integration** J_E**, hence to the pulsating zero-velocity surfaces.**

each other (except for a constant term). By neglecting the integral term, however, the quasi-steady approach creates artificial zero-velocity surfaces which pulsates periodically. This pulsation is an *over-estimation* of either the regions of motion or the forbidden regions. Even if the third body is in equilibrium at $L1$, for instance, we can find forbidden regions that include the current position of the spacecraft $L1$, or regions of motion that open up at $L2$.

Forbidden Subregions, Subregions of Motion and Low-Velocity Subregions

We propose an alternative approach which yields the definition of under-estimated regions of motion and forbidden regions. In between them we define a region which include the zero-velocity surfaces which we call low-velocity region .

First we note that the integral term $I(f; f_0)$ has local minima and maxima at each planet pericen-

ter and apocenter respectively. In fact[§]:

$$\frac{dI}{df} = 0 \rightarrow \bar{f} = n\pi \tag{6}$$

and:

$$\left.\frac{d^2 I}{df^2}\right|_{f=n\pi} = (-1)^n k \quad (k > 0) \tag{7}$$

Hence even if the integral term cannot be computed without the knowledge of the full solution $\mathbf{x}(t)$, we can still evaluate its upper and/or lower boundaries for any finite interval of true anomaly.

If the initial condition $\mathbf{x}_0$ is given at $f_0 = 0$, Eq. (6) and Eq. (7) imply $I(f; f_0) \geq 0$ for all $f \in [-\pi, \pi]$. We can then define the subset

$$\mathcal{F}_f^* \subset \mathcal{F}_f, \ \mathcal{F}_f^* = \left\{(x, y, z) | (2\Omega_C - A - J_E^p) < 0\right\}$$

with $J_E^p = J_E(0, \mathbf{x}(0))$. We call the subset $\mathcal{F}_f^*$ forbidden subregion of motion, as it represents an under-estimation of the forbidden region. The forbidden subregions give useful information in the entire interval $[-\pi, \pi]$. Because they shrink and expand as the true anomaly f goes from $-\pi$ to 0 and from 0 to π (their boundaries are defined by the same equation of the pulsating curves). We use them to formulate a necessary condition for transfer trajectories in the ER3BP:

Given a set of initial condition $f_0 = 2n\pi$; $\mathbf{x_0} = \mathbf{x}(f_0)$, a transfer trajectory between the primaries cannot occur in the interval $[2n\pi - \pi, 2n\pi + \pi]$ if $L1 \in \mathcal{F}_{(2n-1)\pi}^*$ and $L1 \in \mathcal{F}_{(2n+1)\pi}^*$.

Similarly, given a set of initial condition $f_0 = \pi$; $\mathbf{x_0} = \mathbf{x}(\pi)$, Eq. (6) and Eq. (7) imply $I(f; f_0) \leq 0$ for all $f \in [0, 2\pi]$. We define the subregions of motion

$$\mathcal{A}_f^* \subset \mathcal{A}_f, \ \mathcal{A}_f^* = \left\{\mathbf{x} | (2\Omega_C - A - J_E^a) > 0\right\}$$

with $f \in [0, 2\pi]$ and $J_E^0 = J_E(0, \mathbf{x}(0))$.

Finally, if we know the state $\mathbf{x}$ at two consecutive apsidal positions of the primaries we can compute both J_E^a and J_E^p, hence the low-velocity subregions

$$\mathcal{L}_f^* = \left\{(x, y, z) | (2\Omega_C - A - J_E^p) > 0, (2\Omega_C - A - J_E^a) < 0\right\}$$

This set is the complement to the subregions of motion and the forbidden subregions, and by definition it includes the zero-velocity surfaces. For true anomaly intervals $[f_L, f_U] \subset [0, 2\pi]$ we can still define low-velocity surfaces, by replacing J_E^p and J_E^a with $J_E^L = J_E(f_L)$ and $J_E^U(f_U)$.

Figure 6 show the subregions of motion on the xy plane of a third body in the Earth-Moon ER3BP ($e = 0.054$, $\mu = 0.0123$) in the interval $[0, 2\pi]$. The third-body is on a small quasi-periodic orbit around $L1$. In this case the low-velocity subregions always include the quasi-periodic orbit.

[§]Assuming $\left|\frac{d\Omega^*}{df}\right| < \infty$
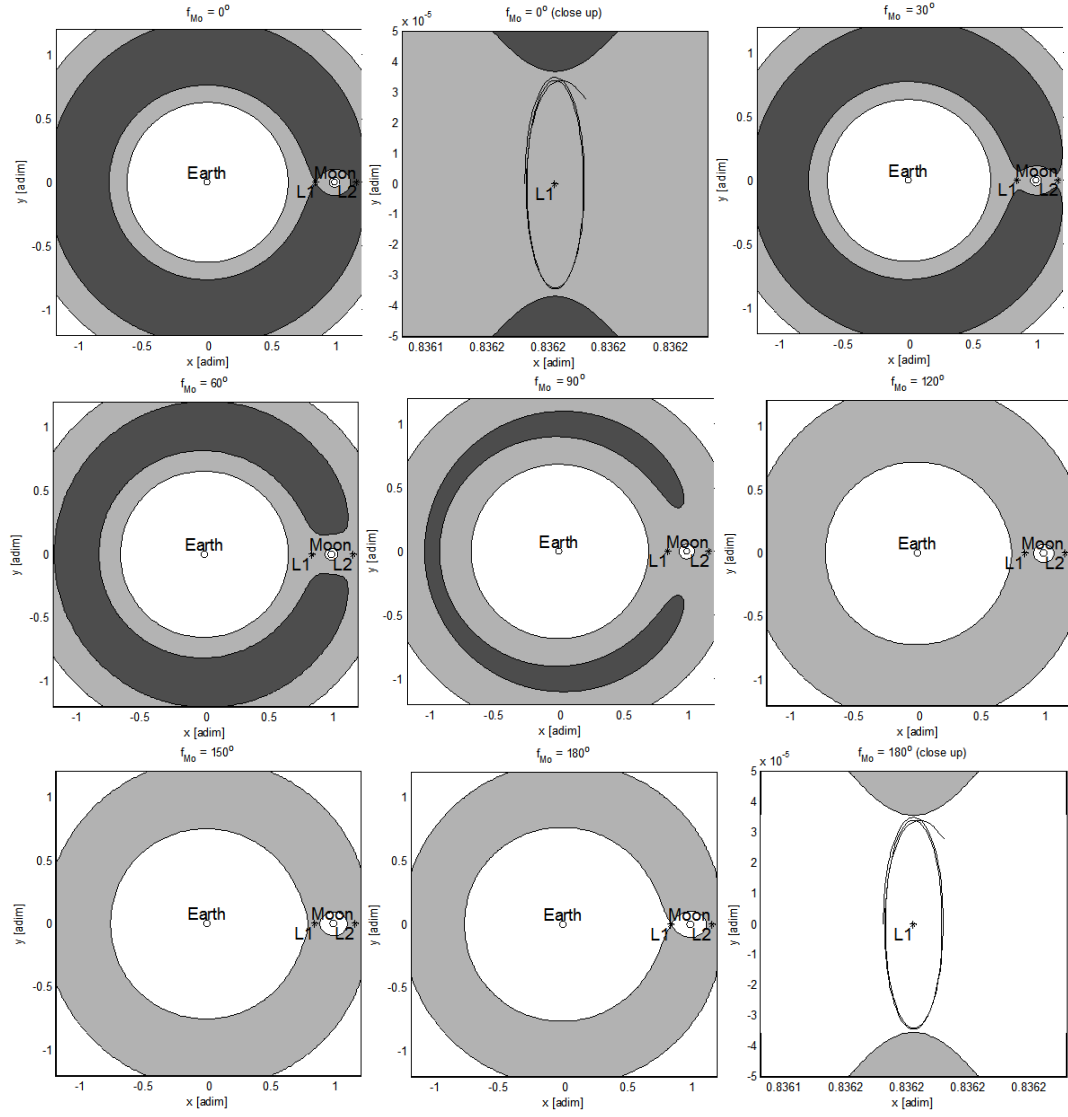
Figure 6 **Subregions of motion for a third body on a small** $L1$ **quasi-periodic orbit of the Earth-Moon ER3BP.** f_{Mo} **is the true anomaly of the Moon. The subregions of motion are plotted each** 30° **of true anomaly of Mercury. The white region is the subregion of motion. The dark gray region is the forbidden subregion. The light gray region is the low-velocity region.**

PERIODIC ORBITS

In this section we show how to compute periodic orbits in the ER3BP. In particular, we compute and study the stability of some orbits which we call *elliptic halo orbits* since they bifurcate from special halo orbits of the CR3BP. We first introduce the periodic orbits in the ER3BP.

The right hand side of the equations of motion Eq. (3) is periodic with period 2π. Thus, periodic solutions of the ER3BP must have principal period $T = 2N\pi$, $N = 1, 2, \ldots$; they are also periodic in the inertial reference frame. In the context of the *planar* ER3BP, Moulton[14] used these considerations and the symmetry properties of the system Eq. (3) to formulate the Strong Periodicity

Criterion :

For an orbit to be periodic [in the planar ER3BP] it is sufficient that it has two perpendicular crossing with the syzygy-axis, and that the crossings happen at moments when the two primaries are at an apse, (i.e. , at maximum or minimum elongation, or apoapsis and periapsis).

In the late 1960es Broucke[15] used Moulton's criterion to compute planar orbits in the ER3BP. He chose 150 orbits of the planar CR3BP with period $T = 2N\pi$ as starting points, with $N = 1, 2, 3, 4, 5$, and computed them in the planar ER3BP for different eccentricities using a continuation method. In particular, each of the 150 orbits was continued into two branches of orbits, which he called periapsis orbits and apoapsis orbits, depending on the true anomaly of the primaries at the starting point on the syzygy axis ($f = 0$ or $f = \pi$).

We use a similar approach to compute elliptic halo orbits. We extend Moulton's criterion and Broucke's approach as the elliptic halo orbits are 3D and in general have periods smaller than 2π. First we consider the following symmetries of the system Eq. (3):

$$S1 : (k\pi + f, x, y, z, \dot{x}, \dot{y}, \dot{z}) \rightarrow (k\pi - f, x, -y, -z, -\dot{x}, \dot{y}, \dot{z})$$

$$S2 : (k\pi + f, x, y, z, \dot{x}, \dot{y}, \dot{z}) \rightarrow (k\pi - f, x, -y, z, -\dot{x}, \dot{y}, -\dot{z})$$

which we use to formulate the Elliptic Periodicity Conditions:

For an orbit to be periodic in the ER3BP, it is sufficient that it has two perpendicular crossing with either the normal plane *(from S1) or the* syzygy axis *(from S2), or both of them, when the primaries are at an apse .*

Second, we choose halo orbits with principal period $T_C = 2r\pi$, where $r = \frac{N}{M}$ is the resonant ratio between the number of the primary revolutions N and number of the third body revolutions M. By assembling M revolutions of a halo orbit, we build an orbit with period $T_E = MT_C = 2N\pi$ which is a solution of Eq. (3) for $e = 0$, and which has $2M$ perpendicular crossings with the normal plane (M left x-intercepts and M right x-intercepts).

If the first crossing of the orbit occurs when the primaries are an apse, then the $M + 1$th crossing also occurs when the primaries are at an apse. More precisely, the $M + 1$th crossing occurs $N\pi$ after the first crossing. Such orbit is an elliptic halo orbit for $e = 0$, and satisfies the Elliptic Periodicity Condition as it has two perpendicular crossing with the normal plane when the primaries are at an apse. Next we compute elliptic halo orbits for $e > 0$ using the eccentricity as a continuation parameter and we impose a perpendicular crossing on the 1st and on the $M + 1$th intercepts at fixed times.

Different kinds of elliptic halo orbits can be assembled starting from the same halo orbit in the CR3BP. For instance, if M is odd we can compute periapsis or apoapsis families depending on whether the first crossing occurs at the periapse or apoapse as described by Broucke for $M = 1$.[15] However, if M is even we can continue two new families of orbits, which we call the left and right family, depending on whether the first crossing is a left x-intercept or a right x-intercept.

We apply our approach to two different cases. In the first case, we consider a system with a small mass ratio $\mu \approx 1e - 6$, corresponding to the Mercury-Sun system, and choose as $L1$ halo orbit with $T_C = \frac{4}{5}\pi$, i.e. $N = 2$ and $M = 5$. We build the elliptic halo orbit by assembling five revolutions

of the halo orbit ($T_E = 4\pi$), and we compute the periapsis and apoapsis families for eccentricities up to $e \approx 0.02$. Figure 7 shows the two families, in both the rotating and inertial reference frames. We also compute an orbit of the pericenter family for $e \approx 0.2$, corresponding to the eccentricity of Mercury's orbit, and compare our solution to one integrated with the full ephemeris model - see Figure 1.
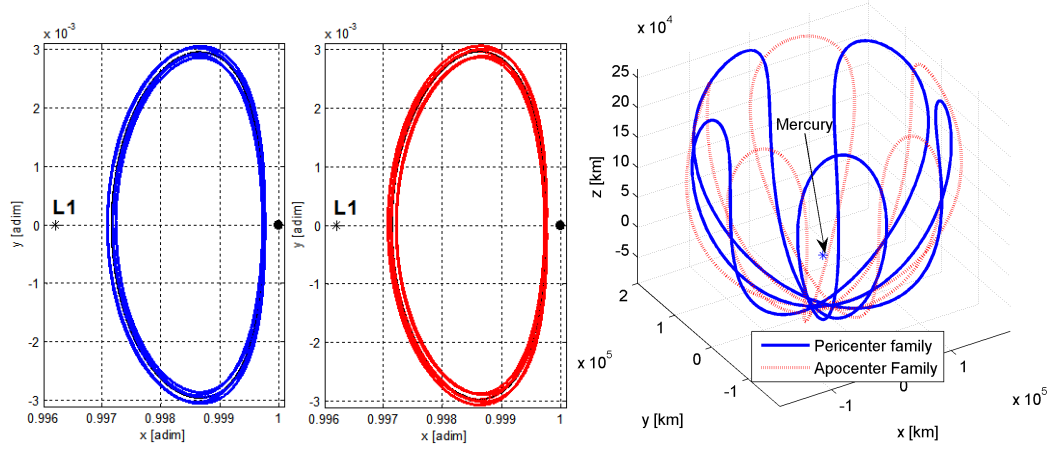
Figure 7 **Periapsis and apoapsis elliptic halo orbits in the ER3BP ($e = 0.02$) generated from a 2:5 halo orbit in the CR3BP. The first and second figure from the left show the periapsis and apoapsis halo orbits in the rotating reference frame. The last figure shows both orbits in the inertial reference frame.**
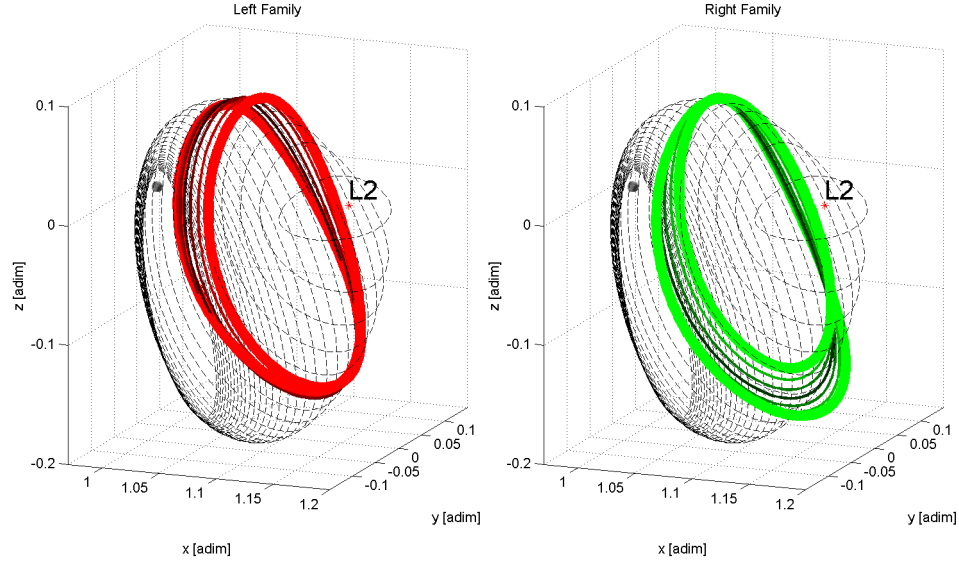
Figure 8 **Left and Right elliptic halo orbits in the ER3BP ($0 < e < 0.3$, $\mu \approx 0.0123$). The dash lines are the L2 halo orbits in the CR3BP. The bold solid line is the elliptic halo for $e = 0.3$. On the Left: 'Left' family that bifurcates from the L2 halo in the pulsating reference frame. On the Right: 'Right' family that bifurcates from the L2 halo in the pulsating reference frame.**

In the second case, we consider a system with a relatively high mass ratio: $\mu = 0.012$, similar to the Earth-Moon system, and choose a halo orbit orbit with period $T_C = \pi$, i.e. $N = 1$ and $M = 2$. We build the elliptic halo orbit by assembling two revolutions of the halo orbit, and we compute the left and the right elliptic halo orbits for eccentricity up to $e = 0.3$. Note that when continuing the orbit from $e = 0$ to $e > 0$, the principal period of the elliptic halo orbits changes from T_C to $T_E = 2T_C$. Also one single halo orbit generates two new elliptic halo orbits. Those elements suggest that a period doubling bifurcation occurs at $e = 0$. In the next section we show that the stability properties of the left and right elliptic halo orbits differ from those of the originating halo orbit. Figure 8 shows the left and right families together with the family of halo orbits at $e = 0$. Each color corresponds to an elliptic halo orbit computed with a distinct eccentricity.

Stability

In order to study the linear stability of the elliptic halo orbits, we briefly recall some important results of Floquet's theory. Consider a system of equations:

$$\dot{\mathbf{y}}(t) = A(t)\mathbf{y}(t) \tag{8}$$

where $A(t)$ is periodic with period T, and $\mathbf{y} \in \mathbb{R}^n$. Also consider a fundamental matrix $\psi(t)$ for the system Eq. (8), and the matrix $E = \psi(0)^{-1}\psi(T)$ [¶]. If E has n distinct eigenvalues λ_i, then there are n solutions $\mathbf{y}_i(t) = \mathbf{q}_i(t)e^{\rho_i(t+T)}$, where $\mathbf{q}_i(t)$ are periodic function with period T, and ρ_i are the characteristic exponents associated to λ_i. Also, it can be shown that $\mathbf{y}_i(t + T) = \lambda_i\mathbf{y}_i(t)$, and the eigenvalues λ_i determine the stability properties of the system Eq. (8).

We can now apply Floquet's theory to the ER3BP. The linearized first order system of ODEs is:

$$\delta\dot{\mathbf{x}}(f) = A(f)\delta\mathbf{x}(f)$$

where

$$A(f) = \begin{bmatrix} 0 & I \\ \frac{\partial^2 \omega_E}{\partial \mathbf{r}^2} & 2J \end{bmatrix}$$

and:

$$
\begin{aligned}
\frac{\partial^2 \omega_E}{\partial \mathbf{r}^2} &= \frac{\partial^2 \Omega_C}{\partial \mathbf{r}^2} - \frac{e \cos f}{1 + e \cos f}\frac{\partial^2 \Omega^*}{\partial \mathbf{r}^2} = \\
&= \frac{3\frac{1-\mu}{r_1^3}\hat{\mathbf{r}}_1 \otimes \hat{\mathbf{r}}_1 + 3\frac{\mu}{r_2^3}\hat{\mathbf{r}}_2 \otimes \hat{\mathbf{r}}_2 + (1 - \frac{1-\mu}{r_1^3} - \frac{\mu}{r_2^3})\underline{\underline{I}}}{1 + e \cos f} - \mathbf{e_z} \otimes \mathbf{e_z}
\end{aligned}
$$

The state transition matrix $\phi(f)$ is solution of the system:

$$\dot{\phi}(f) = A(f)\phi(f) \quad \phi(f_0) = I$$

[¶]Assume $t_0 = 0$

In the ER3BP $\phi(f)$ is in fact a fundamental matrix $\psi(t)$ for the system, and the matrix E is the monodromy matrix $M = \phi(T)$ and can be computed by integrating $\phi(f)$ or by using approximation methods.[16] As mentioned in the previous section, the eigenvalues of the monodromy matrix M still come in reciprocal pairs, but there are no more unitary eigenvalues[17] associated to perturbation $\delta\mathbf{x}$ tangent to the trajectory. In the case of the left elliptic halo orbits of Figure 8 on the left, the eigenvalues move on the unit circle, hinting at the existence of quasi-periodic orbits. In the case of the right elliptic halo orbits of Figure 8 on the right, the eigenvalues move on the real axis generating new stable and unstable manifolds; the stability properties of the halo orbits changes when the eccentricity is $e \neq 0$.
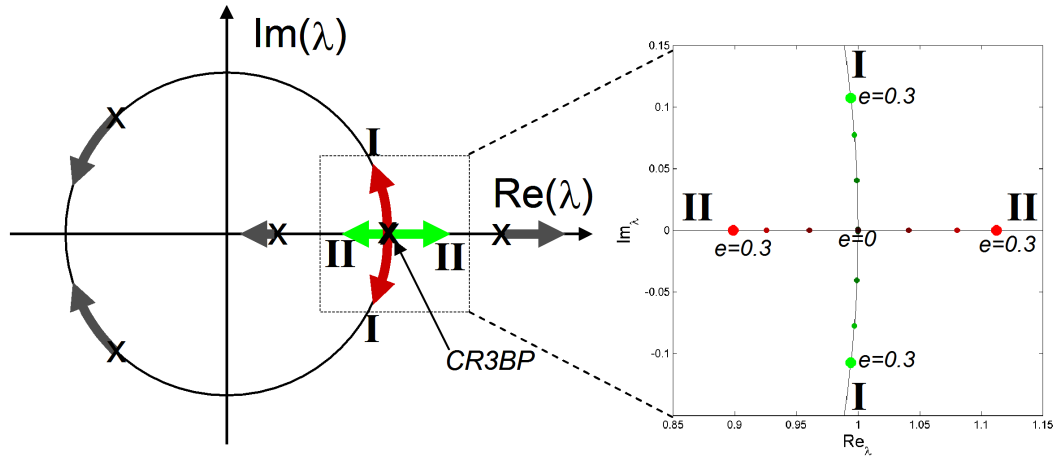
Figure 9 **The real unitary eigenvalues of the halo orbit change as the eccentricity changes. A pair of complex conjugated eigenvalues on the unit circle is generated in the case of the left elliptic halo orbits (branches I), while a stable/unstable pair of eigenvalues is generated in the case of the elliptic right halo orbits (branches II). The left picture is schematic, while the right is the result of the numeric computation.**

CONCLUSIONS

In this paper we defined several regions of motion and periodic orbits in the ER3BP. The Hill's zero-velocity surfaces in the CR3BP are replaced by the low-velocity regions, which divides the subregions of motion from the forbidden subregions. Periodic trajectories are computed using a continuation method, starting with orbits in the CR3BP with period synchronous to the period of the primaries. We showed that different branches of periodic orbits bifurcates in the ER3BP and that the new branches have different linear stability properties.

ACKNOWLEDGMENT

REFERENCES

[1] R. Jehn, S. Campagnola, D. Garcia, and S. Kemble, "Low-Thrust Approach and Gravitational Capture at Mercury," *18th International Symposium on Space Flight Dynamics*, Vol. 548 of *ESA Special Publication*, 2004, p. 487.

[2] W. S. Koon, M. W. Lo, J. E. Marsden, and S. D. Ross, "Heteroclinic Connections between Periodic Orbits and Resonance Transitions in Celestial Mechanics," *Chaos*, Vol. 10, pp. 427–469.

[3] J. F. Palaciána, P. Yanguasa, S. Fernández, and M. A. Nicotra, "Searching for Periodic Orbits of the Spatial Elliptic Restricted Three-Body Problem by Double Averaging," *Physica D: Nonlinear Phenomena*, Vol. 213, 2006, pp. 15–24.

[4] S. Campagnola and M. Lo, "BepiColombo Gravitational Capture and the Elliptic Restricted Three- Body Problem," *Proceedings in Applied Mathematics and Mechanics*, 2007.

[5] V. Szebehely, *Theory of orbits. The restricted problem of three bodies.* New York: Academic Press, 1967.

[6] G. W. Hill, "Researches in the Lunar Theory.," *American Journal of Mathematics*, Vol. 1, No. 1,2, 1878, pp. 5–26, 129–147, 245–260.

[7] H. Poincaré, *Les Méthodes Nouvelles de la Mécanique Celeste.* Paris, Gauthier-Villars et fils, 1892.

[8] K. R. Meyer, *Periodic Solutions of the N-Body Problem.* Springer-Verlag, 1999.

[9] C. C. Conley, "Low Energy Transit Orbits in the Restricted Three-Body Problem.," *Journal on Applied Mathematics*, Vol. 16, 1968, pp. 732–746.

[10] J. V. Breakwell and J. V. Brown, "The 'halo' family of 3-dimensional periodic orbits in the earth-moon restricted 3-body problem," *Celestial Mechanics*, Vol. 20, Nov. 1979, pp. 389–404.

[11] G. Gómez, "Effect of mass-parameter on the periodic orbits of the restricted problem of three bodies.," *Instabilities in dynamical systems*, 1979, pp. 285–286.

[12] K. C. Howell, "Three-dimensional, Periodic, 'Halo' Orbits," *Celestial Mechanics*, Vol. 32, 1984, pp. 53–71.

[13] G. W. Deodel, V. A. Romanov, R. C. Paffenroth, H. B. Keller, D. J. Dichmann, J. Galán-Vioque, and A. Vanderbauwhede, "Elemental Periodic Orbits Associated with the Libration Points in the Circular Restricted 3-Body Problem," *International Journal of Bifurcation and Chaos in Applied Sciences and Engineering*, Vol. 17, No. 8, 2007, pp. 2625–2678.

[14] F. R. Moulton, D. Buchanan, T. Buck, F. L. Griffin, W. R. Longley, and W. D. MacMillan, *Periodic Orbits.* Washington, Carnegie institution of Washington, 1920.

[15] R. Broucke, "Stability of Periodic Orbit in the Elliptic, Restricted, Three-body problem," *AIAA Journal*, Vol. 7, 1969, pp. 1003–1009.

[16] P. Gurfil and D. Meltzer, "Semi-Analytical Method for Calculation the Elliptic Restricted Three-Body Problem Monodromy Matrix," *Journal of Guidance*, Vol. 30, 2007, pp. 266–271.

[17] R. Broucke, H. Lass, and D. Boggs, "A note on the solution of the variational equations of a class of dynamical system," *Celestial Mechanics*, Vol. 14, 1976, pp. 383–392.